Multifunctional Luminescent Down-Shifting Fluoropolymer Coatings: A Straightforward Strategy to Improve the UV-Light Harvesting Ability and Long-Term Outdoor Stability of Organic Dye-Sensitized Solar Cells

Gianmarco Griffini, Federico Bella, Filippo Nisic, Claudia Dragonetti, Dominique Roberto, Marinella Levi, Roberta Bongiovanni, and Stefano Turri*

Received: July 31, 2014
Revised: September 2, 2014
Published online: September 29, 2014

1. Introduction

Dye-sensitized solar cells (DSSCs) have gained increasing attention in the past two decades as a next generation photovoltaic (PV) technology alternative to conventional silicon (Si)-based systems because of their potentially low fabrication costs, ease of preparation and relatively high light-to-electricity energy conversion efficiencies.[1,2]

Highly performing DSSCs conven-tionally incorporate sensitizers based on polypyridyl ruthenium (Ru) complexes that can give power conversion efficien-cies in excess of 11%.[3] Despite their great potential, Ru-based sensitizers suffer from issues related to the high costs, toxicity and limited availability of the starting mate-rial, thus making them not suitable for a widespread application in cost-effective and environmentally friendly DSSC sys-tems.[4] In the attempt to overcome some of these limitations, several metal-free organic dyes have been synthesized in the past few years,[5–7] among which indoline-based sensitizers have shown DSSC device effi ciencies approaching those obtained with conventional Ru-based complexes.[8]Common to all organic systems is the relatively narrow absorption response,[9] that inevitably limits optimal utilization of the solar spectrum and thus device effi ciency. Different strategies have been proposed to broaden the light-harvesting ability of

DSSC devices, including the use of two or more sensitizers with complementary absorption spectra,[10–12] the doping of the TiO_2 photoanode with a UV-excited lumi-nescent compound[13] and the use of tandem devices.[14–16] Although promising, all these approaches present several technical and fabrication challenges that limit their widespread practical applicability.[17,18]

In recent years, luminescent down-shifting (LDS) has re-emerged as a convenient and technologically viable strategy

Dr. G. Griffini, Prof. M. Levi, Prof. S. Turri
Department of Chemistry, Materials and Chemical Engineering "Giulio Natta"
Politecnico di Milano
PiazzaLeonardodaVinci32 , 20133 Milano, Italy
E-mail: gianmarco.griffini@polimi.it
F. Bella, Prof. R. Bongiovanni
Department of Applied Science and Technology – DISAT
Politecnico di Torino
CorsoDucadegliAbruzzi24 , 10129 Torino, Italy

F. Bella
Center for Space Human Robotics @Polito
Istituto Italiano di Tecnologia
Corso Trento 21, 10129 Torino, Italy
Dr. F. Nisic, Dr. C. Dragonetti, Prof. D. Roberto
Department of Chemistry
Università degli Studi di Milano
Via Golgi 19, 20133 Milano, Italy

to extend the short-wavelength limit of solar cells through the absorption of incident UV-photons and their re-emission at longer wavelengths, where the PV photoactive materials typically show optimal spectral response.[19] Conventional LDS systems involve the application of a luminescent coating on the top of the complete PV device with no interference between luminophore and solar cell active material, thus making this approach extremely flexible and easy to be implemented also on an industrial scale.[20] This technique has been successfully applied to different inorganic PV technologies,[21,22] with Si-based systems being the most widely investigated[23] due to their poor external quantum efficiency (EQE) at short wavelengths. As opposed to this, only a very few reports have been presented on the potential application of LDS to DSSCs, the vast majority of which involving the synthesis and characterization of nanocrystals (NCs) based on lanthanide (Ln) phosphors ($LaVO_4$:Dy^{3+}, Y_2WO_6:Ln^{3+}/Bi^{3+}, Gd_2MoO_6:Ln^{3+}/Bi^{3+}, YVO_4:Bi^{3+}/Ln^{3+}) as potential down-shifting materials.[24,25] Even less works[17,26] have been reported to date on the actual use of these materials as LDS coatings on functioning DSSC systems with related device performance evaluation. Despite their interesting photophysical properties that can be useful when coupled to DSSC photoactive materials, all these Ln-based NCs require very high sintering temperatures (often in the 500–1000 °C range) for their formation, which inevitably limit their widespread use in commercial DSSC applications.

In addition to maximizing device efficiency, another major and often overlooked aspect to be addressed before envisaging commercial deployment of organic PV technologies such as polymer solar cells and DSSCs is the need of long-term operational stability in outdoor conditions, which are characterized by continuous exposure to the harmful UV portion of the solar spectrum as well as to adverse weather conditions (e.g., rain, snow).[27,28] One of the most straightforward and technologically viable strategies to address this issue is the ex-post application of multifunctional protective coatings on the as-fabricated PV device. Although this technique is quite common and well consolidated in several industrial fields (e.g., automotive, architectural, nautical), only very recently the use of multifunctional protective coatings has been demonstrated in energy conversion and storage systems.[29,30] Furthermore, only a surprisingly small number of these works is focused on DSSC technology, where the combination of self-cleaning and antireflective properties has been proposed as a promising strategy to improve light-harvesting and device stability.[31] Following these very recent examples of multifunctional systems, it would be highly desirable to be able to combine LDS, UV-screening and easy-cleaning properties within a single coating material, to allow the fabrication of DSSCs with optimized spectral management and enhanced device stability in an easily implemented and versatile fashion.

Here, we present the first demonstration of a multifunctional coating that incorporates LDS, UV-screening and easy-cleaning abilities, and its application in Ru-free organic DSSC devices. Such coating consists of a new photocrosslinkable fluorinated polymer embedding a newly synthesized photoluminescent europium (Eu) complex that acts as down-shifting material converting harmful UV photons into valuable visible light (**Figure1** a). By carefully optimizing the concentration of the luminescent species in the fluoropolymeric coating applied on organic DSSC devices, a 70% relative increase in power conversion efficiency was obtained with respect to control uncoated devices. This represents the highest efficiency enhancement reported so far on organic DSSC systems by means of a polymeric LDS layer. In addition, long-term weathering tests revealed the excellent stabilizing effect of our new coating on DSSC devices. For the first time, after more than 2000 h of continuous exposure to real outdoor conditions, DSSCs incorporating the new coating system presented in this work were found to fully preserve their initial power conversion efficiency, as opposed to LDS-free control devices that showed a 30% efficiency loss. This excellent outdoor stability was attributed to the combined action of the luminescent material that acts as UV-screen and the highly photostable, hydrophobic fluoropolymeric carrier that further prevents photochemical and physical degradation of the solar cell components. The results of the present study clearly demonstrate that in the case of organic DSSCs significant performance improvements can be achieved by using the new LDS coating presented in this work, thus bridging the gap with generally better performing (but potentially critical in view of commercial application) Ru-based DSSCs. Nonetheless, due to the high flexibility in the choice of photoactive materials available for DSSC devices, our approach may be extended to a large variety of sensitizer/luminophore combinations with suitable spectral match, thus enabling the fabrication of highly efficient and exceptionally stable DSSC systems.

2. Results and Discussion

The multifunctional coating presented in this work was obtained by ultraviolet (UV)-mediated photocrosslinking of a newly synthesized fluoropolymeric precursor containing a photosensitive methacrylic functionality appended to the main polymeric chain. The preparation of such precursor involved the reaction between a commercial chloro-trifluoro-ethylene vinyl-ether (CTFEVE) polymeric binder and 2-isocyanatoethyl methacrylate (IEM), according to the scheme presented in Figure 1b. Such reaction leads to the formation of a fluorinated polymer bearing methacrylate functionalities as pendant groups linked to the polymeric backbone via urethane bonds resulting from the polyaddition of the –OH groups present in the CTFEVE binder and the –N=C=O group of IEM. The detailed description of the synthetic procedure is presented in the Experimental Section.

The presence of the methacrylate moiety appended to the main polymer chain allows the photocrosslinking reaction under UV-light, leading to the formation of the polymeric solid film. To probe the kinetics and the conversion of the photocrosslinking reaction, Fourier-transform infrared (FTIR) spectra of the cast films were collected at increasing UV-light exposure times and the intensity decrease of the FTIR signal centered at 1636 cm^{-1} (methacrylate C=C stretching) was monitored, normalized with respect to the carbonyl C=O stretching signal at 1720 cm^{-1} (Figure 1c).[32] The conversion (X) of the reactive groups at time t was evaluated by computing the ratio between the intensity of the FTIR signal at 1636 cm^{-1} at a given time t and prior to irradiation. As shown in Figure 1d, a conversion

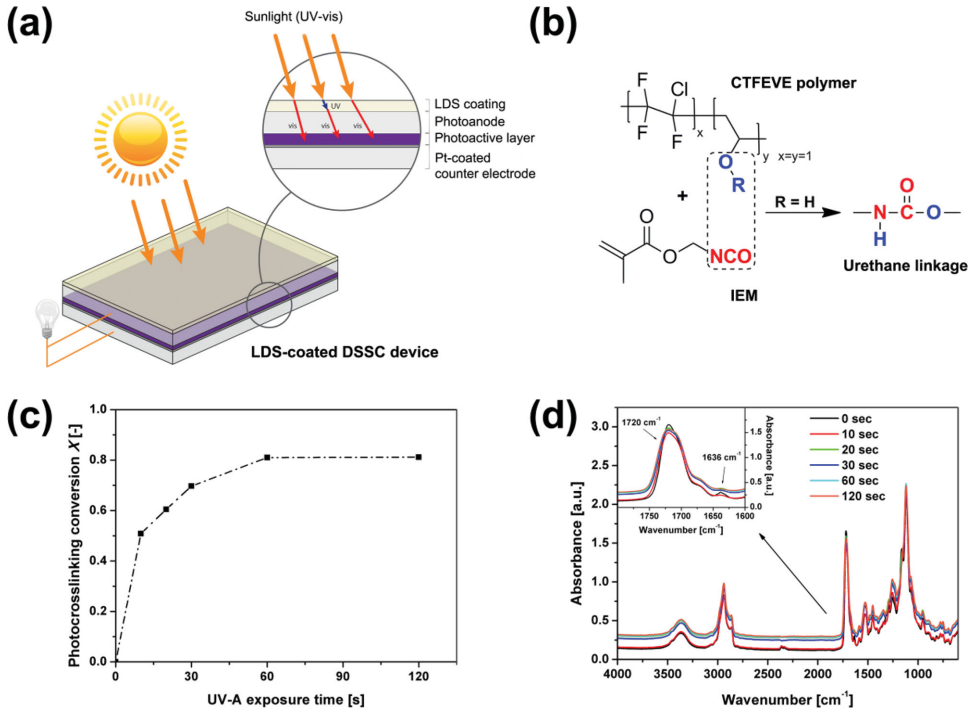

Figure 1. a) Graphical representation of the working principle of the LDS system presented in this work; b) schematic representation of the mechanism of formation of the photocrosslinkable fluoropolymer precursor; c) photocrosslinking conversion curve; and d) FTIR spectrum of the photocrosslinked fluoropolymer at increasing UV-exposure time. The inset shows the region of the FTIR spectra where the C=C stretching signal is observed.

of over 80% is found for this system already after 60 s of UV-light exposure, followed by a plateau which indicates that photocrosslinking was achieved, as also evidenced by the resistance of the UV-cured coatings to solvent rubbing (MEK double rub test).[33] This behavior clearly indicates that an efficient and rapid crosslinking process can be achieved with our new photocrosslinkable system, potentially leading to a straightforward scalability to large production volumes, especially when compared with conventional thermal crosslinking processes, where long exposure times to high temperatures (in the 150–200 °C range) are often needed to complete the curing.[30]

To serve as light-managing LDS layer for DSSC devices, a luminescent species was added to the new fluoropolymeric coating. In this work, europium tetrakis dibenzoylmethide triethylammonium (EuD_4TEA) was chosen as the luminescent material (**Figure 2**a) because of its large Stokes shift and good spectral breadth in the UV region of the solar spectrum, being these characteristics of great importance for DSSC applications. EuD_4TEA was synthesized based on previously published work[34] using a slightly modified procedure (see Experimental Section for details on the synthetic protocol) and was incorporated into the fluoropolymeric precursor prior to photocrosslinking. The optical properties of the LDS coating incorporating EuD_4TEA were examined by means of UV–Vis and fluorescence spectroscopy. As shown in Figure 2c, a broad absorption band is found in the LDS coating covering the 300–400 nm spectral range, with an absorption peak centered at 350 nm. The photoluminescence spectrum shows the characteristic narrow emission bands of Eu(III) corresponding to the $^5D_0 \rightarrow {}^7F_{0-4}$ transitions. In particular, a sharp emission is found at 613 nm resulting from the $^5D_0 \rightarrow {}^7F_2$ electronic transition, while the lower intensity emission peaks at 579 nm, 594 nm, 653 nm and 703 nm are associated with the $^5D_0 \rightarrow {}^7F_0$,

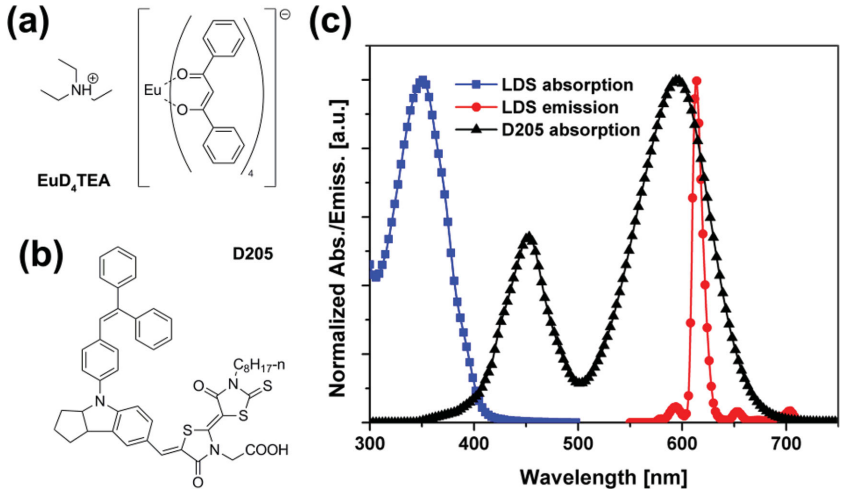

Figure 2. a) Molecular structure of EuD_4TEA; b) molecular structure of D205; and c) normalized UV–Vis and photoluminescence emission spectra of EuD_4TEA-doped LDS coatings and absorption spectrum of D205 deposited on TiO_2.

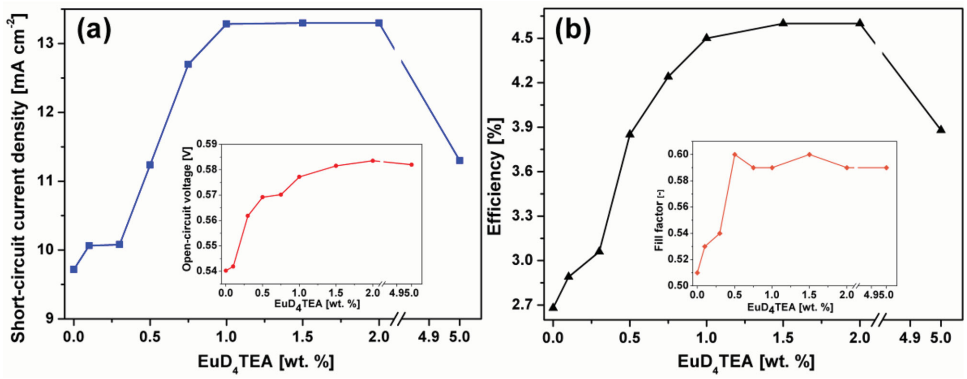

Figure 3. Variation of PV parameters of LDS-coated DSSC devices at increasing concentration of EuD_4TEA luminescent species: a) short-circuit current density J_{sc} and open-circuit voltage V_{oc} (inset), and b) device efficiency η and fill factor FF (inset).

$^5D_0 \rightarrow {}^7F_1$, $^5D_0 \rightarrow {}^7F_3$ and $^5D_0 \rightarrow {}^7F_4$ transitions, respectively.[34] Based on these observations, it is clear that EuD_4TEA represents a very promising candidate as down-shifting material in LDS polymeric coatings for DSSC applications. In order to optimally exploit the interesting optical properties of EuD_4TEA-doped LDS coatings, an appropriate DSSC dye needs to be selected. For this purpose, after a thorough screening we decided to couple the EuD_4TEA-based LDS coating with the Ru-free indoline-based organic dye D205 (Figure 2b),[4,8b] which was recently emphasized for its good PV performance also in the presence of flexible electrodes and alternative redox couples.[35] As clearly evident in Figure 2c, a good match between the emission spectrum of the luminescent material and the absorption spectrum of the dye is present. Furthermore, EuD_4TEA absorbs photons in an area where D205 is not active, thus no competitive optical phenomena are expected to occur.

In order to assess the actual performance of the proposed system, DSSCs were assembled with a D205-sensitized TiO_2 electrode, a iodide/triiodide liquid electrolyte and a Pt-sputtered counter electrode. LDS coatings were deposited on the external side of the photoanode, and the effect of EuD_4TEA concentration in the photopolymer on the performance of the DSSC device was investigated. **Figure 3** shows the strikingly positive effect of the LDS layer on PV cell performance. A remarkable 37% improvement of short circuit current density (J_{sc}, Figure 3a) is already achieved when a 1 wt% EuD_4TEA is introduced in the crosslinked coating. This confirms that the luminescent material can effectively convert the spectral region peaked at 350 nm into lower-energy photons of wavelengths well matching the absorption spectrum of D205. As a result, the increased amount of photons reaching the DSSC dye due to the photoluminescence process occurring in the LDS coating is responsible for the observed improvement in J_{sc}. Further evidence of the proper functioning of the proposed LDS system was given by incident photon-to-current efficiency (IPCE) measurements. Indeed, from **Figure 4** it is clear how the luminescent material leads to increased IPCE values in the spectral region where the absorption of EuD_4TEA is centered (350 nm). In particular, progressively higher IPCE values are observed at increasing EuD_4TEA concentration in the 330–370 nm spectral region, where incoming photons are shifted to the absorption peak of the DSSC sensitizer, thus generating enhanced photocurrent (see Figure S1 in the Supporting Information for the corresponding J–V curves). Integrating the product of the AM1.5G photon flux with the IPCE spectrum yields predicted J_{sc} values equal to 9.79 mA cm^{-2} and 13.08 mA cm^{-2}, for the LDS-free and LDS-coated DSSCs, respectively, which are in excellent agreement with the measured values reported in **Table 1**. The luminescence of the UV-cured coatings can be appreciated in the inset of Figure 4.

While the increase of photocurrent could be reasonably expected in the presence of a LDS system, the insets of Figure 3 show that also V_{oc} and FF were slightly improved with increasing EuD_4TEA concentration. It is well known that these two parameters are usually affected by changes of the electrolyte composition or by modification of the electrodes/electrolyte interfaces.[36] However, the same components were used in our work to fabricate the DSSC devices at varying EuD_4TEA concentration. The only factor that may affect these PV parameters in this case is the operating temperature. Indeed, it has been previously demonstrated that the increase of DSSC device temperature causes a decrease of V_{oc} and FF (due to accelerated recombination reactions) accompanied by a slight increase in J_{sc}, that results in an overall decrease of the PV cell output power and

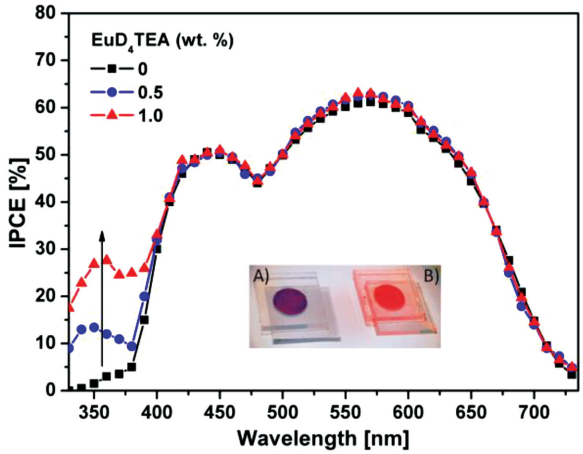

Figure 4. IPCE curves of LDS-coated DSSCs at increasing concentration of the EuD_4TEA luminescent species. The insets show photographs of EuD_4TEA-free (A) and 1 wt% EuD_4TEA-laden (B) DSSCs under UV-light.

Table 1. PV parameters (short-circuit current density J_{sc}, open-circuit voltage V_{oc}, fill factor *FF* and power conversion efficiency η) of LDS-coated (1 wt% EuD_4TEA) and uncoated (0 wt% EuD_4TEA) DSSC devices. The performance decrease after 2140 h of outdoor operation (η_{loss}) is also reported.

EuD_4TEA [wt%]	J_{sc} [mA cm^{-2}]	V_{oc} [V]	FF [–]	η [%]	η_{loss} [%]
0	9.72	0.54	0.51	2.68	28
1	13.29	0.58	0.59	4.50	2

in a lower conversion efficiency.[37] Based on these observations, a possible explanation for the trends observed in this work may be given by considering the ability of the fluoropolymeric LDS coating deposited on the light-exposed face of the photoanode to absorb hot IR photons incident on the DSSC, thus reducing device operating temperature. Indeed, fluoropolymers are characterized by a strong and wide absorption band in the IR region of the electromagnetic spectrum originating from the C-F bond stretching vibration.[38] This characteristics may help limit the thermally activated recombination phenomena that are responsible for decreased performance in DSSC devices with temperature.

The overall trends observed on the PV parameters presented above show that cell efficiency (η, Figure 3b) increases with EuD_4TEA concentration in the LDS coating, leading to a remarkable maximum η enhancement of 70% with respect to the uncoated device (from 2.68% to 4.50%) for EuD_4TEA concentration in the 1–2 wt% range. To the best of our knowledge, this value represents the highest efficiency enhancement reported so far on organic DSSC systems by means of a polymeric LDS layer. This behavior demonstrates the positive effect of our functional coating on device performance, which appears even more interesting considering the economical, rapid and easily up-scalable processes of deposition and light-curing that were employed for its fabrication. Some attempts to further increase the concentration of EuD_4TEA introduced in the LDS coating were also carried out. However, as shown in Figure 3, a plateau η is reached for EuD_4TEA concentrations in the 1–2 wt% range, followed by a η decrease for higher EuD_4TEA loading. This latter effect may be due to the progressively lower solubility of EuD_4TEA in the fluoropolymeric system at increasing concentrations that leads to the formation of aggregates and precipitates (see Figure S2 in the Supporting Information) contributing to the reduction of transmittance of the LDS coating and thus to an overall DSSC device performance decrease.

Ascertained the significantly positive effect of our functional coating on the DSSCs PV performance, a study on device aging was also conducted. As well known in the scientific community, there is no standardized protocol for the evaluation of the stability of DSSCs, and in most cases a study of 500/1000 h in the dark at high temperature or at room temperature under simulated solar irradiation is performed.[39] In the present work, a long-term weathering study was conducted for the first time under real outdoor conditions for about 3 months (2140 h). The DSSC devices were exposed (day and night) in the garden of the IIT building in Turin (45°03′42.0″N, 7°39′48.1″E), located in northern Italy in a humid subtropical climate zone. The highly

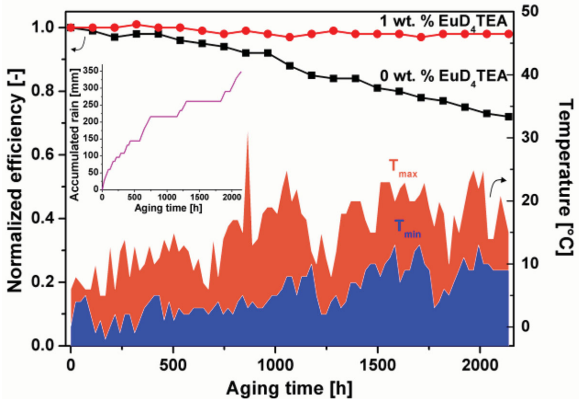

Figure 5. Stability test carried out on LDS-free (0 wt% EuD_4TEA) and LDS-coated (1 wt% EuD_4TEA) DSSCs in real outdoor conditions. The lower part of the graph shows the outdoor temperatures (minimum and maximum) registered during the testing period, while the inset shows the accumulated rainfall.

variable climatic conditions are particularly useful to carry out a realistic study of device aging. As shown in **Figure 5**, outdoor temperatures ranged from –2 to 32 °C during the first quarter of 2014 (between February and April), and about 350 mm of accumulated rain were recorded by the local environmental protection agency.[40] In the considered period, the control DSSC device (0 wt% EuD_4TEA) lost about 30% of its initial efficiency, while the LDS-coated system (1 wt% EuD_4TEA) fully preserved the starting performance, with a minor 2% efficiency loss (Table 1). This remarkable result makes the proposed luminescent fluoropolymeric coating not only useful to produce a great improvement of PV performance, but also to impart high long-term durability in real operating conditions, which is of paramount importance for a practical exploitation of the DSSC technology.

In order to better clarify the striking behavior observed on the stability of LDS-coated systems, further characterizations of the luminescent films were carried out. As regards the thermal properties, differential scanning calorimetry (DSC) was used to evaluate the glass transition temperature (T_g) of the photocrosslinked coating. For outdoor application, the T_g of the fluropolymeric coating should be higher than room temperature so that potential degradation effects due to prolonged outdoor exposure to high temperatures can be prevented. As presented in **Figure 6**a, the EuD_4TEA-free photocrosslinked fluoropolymer shows a T_g value well above room temperature (49 °C), that is further increased upon the addition of the luminescent species (T_g = 59 °C for the LDS coating), indicating a good miscibility between the photopolymer and the luminescent species. These values clearly confirm the suitability of our new LDS coating for outdoor use.

The thermo-oxidative stability of the LDS photocrosslinked coating was investigated by means of thermo-gravimetric analysis (TGA) in air (Figure 6b). A three-stage thermal degradation behavior can be clearly observed, with a first weight loss of about 10–15% occurring in the 150–250 °C, which may be ascribed to cleavage of the urethane bonds.[41] The second major weight loss (60%) is found in the 250–450 °C temperature range that may be due to the decomposition of ether and ester linkages[42]

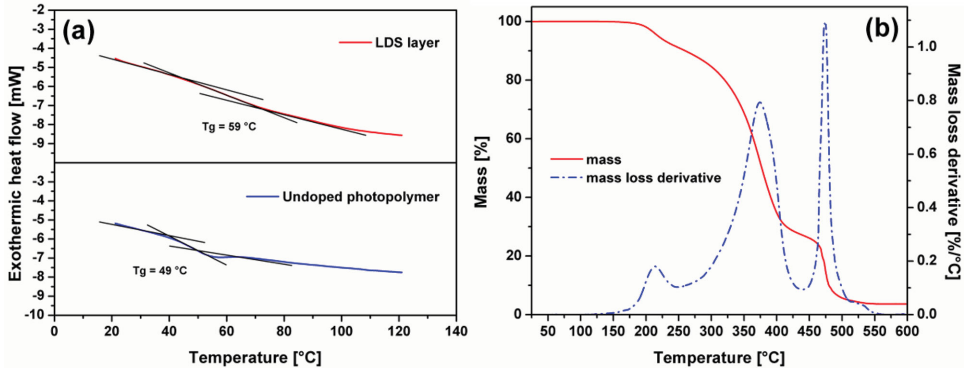

Figure 6. a) DSC curve of undoped and doped photocrosslinked coating and b) TGA thermogram of the LDS coating.

and to chain scission reactions,[43] which are known to occur in acrylate polymers *via* a free-radical mechanism upon heating in air. Finally, the third weight-loss peak observed above 450 °C indicates the complete de-crosslinking and thermal degradation of the polymer. The fluoropolymeric LDS coating presents 5% and 50% weight-loss temperatures of 219 °C and 377 °C, respectively, indicating that the presence of fluorinated units in the polymer backbone imparts excellent thermal stability to the coating for the target application.[44] A similar behavior was found in the EuD_4TEA-free photocrosslinked coating (see Figure S3 in the Supporting Information).

For the purpose of ensuring long-term DSSC lifetime in real outdoor environment, the detrimental action of adverse weather conditions such as rain and snow on device operation needs to be prevented. Therefore, the application of a hydrophobic, low surface-energy polymeric layer on the DSSC device to serve as easy-cleaning protective coating is highly desirable. To investigate the wettability behavior of the new LDS coating, static contact angle measurements were performed using water and diiodomethane as probe liquids, and the surface tension γ of the coating including its dispersive and polar components (γ^d and γ^p, respectively) was calculated using the Wu method.[45] As shown in **Table 2**, the moderately hydrophobic character of the fluorinated LDS coating is evidenced by the evaluation of water contact angle ($\theta_{H2O} = 94.4°$) and surface tension ($\gamma = 36.7$ mN/m). These properties lead to a considerable change in the wettability of the external side of the photoanode upon deposition of the LDS layer, providing an additional easy-cleaning functionality to the LDS coating that may enhance DSSC device lifetime during long-term outdoor operation, as evidenced in Figure 5. In addition to keeping the photoanode clean, thus avoiding the decrease in J_{sc} caused by the formation of physical barriers preventing solar photons from reaching the photoactive components of the device, the chemical nature of the hydrophobic fluorinated LDS coating is expected to prevent one of the main degradative phenomena observed in DSSC from occurring, namely water permeation. Indeed, the introduction of water in DSSC devices is known to cause desorption of the sensitizer,[46] phase separations between polar and apolar electrolyte components[47] and formation of iodate (IO_3^-) from I_3^- ions.[48] In light of this, the use of a hydrophobic coating ensures an efficient protective barrier against atmospheric water. Visual inspection of LDS-coated and control devices after prolonged outdoor exposure further highlighted the easy-cleaning ability and physical barrier properties of the LDS coating that prevents dust particles, dirt and water to deposit on the outer surface of the DSSC device (see Figure S4 in the Supporting Information).

Finally, the luminescent species EuD_4TEA in the multifunctional LDS coating acts as a UV filter, due to its absorption in the 300–400 nm range and its re-emission in the visible light spectrum. This umpteenth positive aspect further explains the exceptional stability observed on LDS-coated devices upon outdoor exposure and makes the here proposed system very efficient in preventing DSSC aging, in particular by reducing the photo-oxidative degradation of the organic sensitizer.[49]

Table 2. Static contact angles (θ_{H2O}, θ_{CH2I2}), total surface tension (γ) and its dispersive (γ^d) and polar (γ^p) components for bare glass and glass coated with LDS photocrosslinked film.

	θ_{H2O} [°]	θ_{CH2I2} [°]	γ [mN m^{-1}]	γ^d [mN m^{-1}]	γ^p [mN m^{-1}]
Bare glass	12.7 ± 2.3	58.6 ± 0.7	71.7 ± 0.7	27.3 ± 0.8	44.4 ± 0.5
LDS-coated glass	94.4 ± 1.1	49.4 ± 1.1	36.7 ± 0.5	33.1 ± 0.3	3.6 ± 0.3

3. Conclusion

In summary, a multifunctional coating system was developed in this work incorporating LDS, UV-screening and easy-cleaning functionalities, for use in Ru-free organic DSSC devices. The new coating consists of a UV-curable fluoropolymer containing a luminescent Eu complex that acts as down-shifting material to convert UV photons into valuable visible light. After careful optimization of the concentration of the luminescent species in the fluoropolymer, DSSC devices incorporating the new coating system were found to show a 70% relative increase in power conversion efficiency as compared with control uncoated devices. To the best of our knowledge, this represents the highest efficiency enhancement reported to date on organic DSSC devices by means of a polymeric LDS layer. In addition, a long-term three months weathering study was performed on operating DSSC devices under real outdoor conditions. DSSCs incorporating the new coating developed in this work were found to fully preserve their initial power conversion efficiency, as opposed to control devices that showed a ≈30% relative efficiency loss. The remarkable outdoor stability found in coated

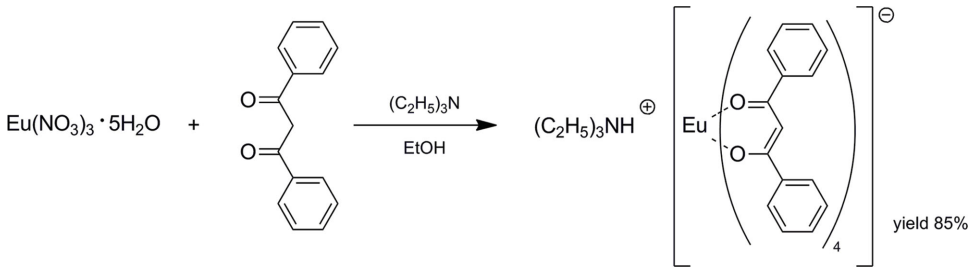

Scheme 1. Synthesis of europium tetrakis dibenzoylmethide triethylammonium (EuD_4TEA).

DSSCs was attributed to the combined action of the luminescent material that acts as UV-screen and the intrinsically photostable, hydrophobic fluoropolymer used as carrier material that further prevents photochemical and physical degradation of the solar cell components. The general approach presented in this study to simultaneously improve performance and weatherability of organic DSSC devices may be readily extended to a large variety of sensitizer/luminophore combinations with appropriate spectral match, thus enabling the fabrication of highly efficient and extremely stable DSSC systems in an easy and versatile fashion.

4. Experimental Section

Photocrosslinkable Fluorinated Precursor: A commercial chloro-trifluoro-ethylene vinyl-ether (CTFEVE) polymeric binder (Lumiflon LF-910LM, Asahi Glass Company Ltd.) was used as the polyol (see Figure S5 in the Supporting Information for the chemical formula) for the reaction with 2-isocyanatoethyl methacrylate (IEM, Showa Denko K.K.), to form the photocrosslinkable polyurethane precursor. CTFEVE (40 g) and IEM (7.3 g) were successively poured in stoichiometric ratio (OH/NCO = 1) into a three-necked round-bottomed flask equipped with a bubble condenser, followed by the addition of di-*n*-butyltin dilaurate (0.3 wt% on IEM). The reaction was conducted at 75 °C under vigorous magnetic stirring and nitrogen atmosphere. The reaction was monitored by means of FTIR spectroscopy by evaluating the disappearance of the N=C=O stretching signal (2270 cm^{-1}) in the FTIR spectrum of the reaction mixture. Complete disappearance of the 2270 cm^{-1} FTIR signal was observed after about 6 h, indicating that the reaction between the OH groups in CTFEVE and NCO groups in IEM was completed. The final product was diluted with chloroform ($CHCl_3$) to the desired concentration.

Europium Tetrakis Dibenzoylmethide Triethylammonium (EuD_4TEA): All materials were provided by Sigma-Aldrich, unless otherwise stated. The synthesis was performed based on a previous work by Fontenot et al.[34] with slight modifications, as shown in **Scheme 1**. Europium nitrate pentahydrate (330 mg, 0.77 mmol) and triethylamine (1 mL, 7.21 mmol) were added to a hot solution of dibenzoylmethane (700 mg, 3.125 mmol) in absolute ethanol (15 mL). The solution was heated until the mixture was clear (ca. 1 h), and then kept aside to cool down slowly overnight. The crystals that formed upon cooling were collected under suction and washed with 5 mL of ethanol. The crystalline product was then air dried, to give the product as a pale yellow solid (758 mg; yield 85%). Characterization of the compound was in agreement with data reported in the literature.

Photocrosslinking Process: Photocrosslinking was carried out by irradiating the photocrosslinkable precursor with a medium pressure mercury lamp equipped with an optical guide (LC8, Hamamatsu) for 60 s under an irradiation intensity of 35 mW cm^{-2} (measured with a UV Power Puck II radiometer, EIT). The UV treatment was performed in a custom-built chamber under nitrogen flux, to prevent quenching of free-radicals by atmospheric oxygen. Darocur 1173 (Ciba Specialty Chemicals) was used as the photoinitiator (3 wt%). As a preliminary test to evaluate the extent of photocrosslinking, the UV-exposed polymer films were immersed into $CHCl_3$ for 5 min and then dried under a stream of nitrogen to check their resistance to solvent washing.[50] In order to monitor the conversion of the photocrosslinking reaction upon UV-light exposure, a film of polymer precursor was deposited onto a KBr disk *via* spin-coating and subsequently irradiated with the UV lamp for a given amount of time, immediately followed by quenching in an ice bath to stop the crosslinking reaction. The FTIR spectrum of the film was then collected. This procedure was repeated on the same polymer film for increasing UV-light exposure times, for a maximum of 120 s.

Fabrication of DSSC Device: Conducting glass plates (FTO glass, fluorine-doped tin oxide over-layer, sheet resistance 7 Ω sq^{-1}, purchased from Solaronix) were cut into 2 cm × 2 cm sheets and used as substrates for both the deposition of a TiO_2 porous film from a paste (DSL 18NR-AO, Dyesol) and the fabrication of platinized counter-electrodes. Sensitizing dye 5-[[4-[4-(2,2-diphenylethenyl)phenyl]-1,2,3,3a,4,8b-hexahydrocyclopent[*b*]indol-7-yl]methylene]-2-(3-octyl-4-oxo-2-thioxo-5-thiazolidinylidene)-4-oxo-3-thiazolidineacetic acid (D205) was purchased from Inabata Europe S.A. All of the other materials were provided by Sigma-Aldrich.

As regards the photoanodes preparation, FTO covered glasses were rinsed in acetone and ethanol in an ultrasonic bath for 10 min. A TiO_2 paste layer with a circular shape was deposited on FTO by screen printing technique (AT-25PA, Atma Champ Ent. Corp.) and dried at 100 °C for 10 min on a hot plate. A sintering process at 525 °C for 30 min led to a nanoporous TiO_2 film with an average thickness of 9 μm, measured by profilometry (P.10 KLA-Tencor Profiler). The photoelectrodes were then soaked into a 0.5 mM D205 dye solution in a *tert*-butanol:acetonitrile 1:1 mixture for 5 h at ambient temperature, and finally washed with acetone to remove the unadsorbed dye. 0.5 mM of chenodeoxycholic acid (CDCA) as coadsorbent in the dye solution was added. As for the counter electrodes, 5 nm Pt thin films were deposited by sputtering (Q150T ES, Quorum Technologies Ltd) onto FTO glasses, previously cleaned with the same rinsing method described above.

Photoanode and counter electrode were assembled into a sealed sandwich type cell with a gap of a hot-melt ionomer film, Surlyn (60 μm, Du-Pont). The cell internal space was filled with electrolyte via vacuum backfilling. The electrolyte consisted of 1-methyl-3-propylimidazolium iodide (MPII, 0.60 M), iodine (I_2, 50 mM), lithium iodide (LiI 0.10 M) and 4-*tert*-butylpyridine (TBP, 50 mM) in 3-methoxypropionitrile (MPN). The injection hole on the counter electrode was finally sealed with a Surlyn sheet and thin glass by heating.

UV-curable reactive mixtures were prepared at a concentration of 30 wt% in $CHCl_3$ following the procedure outlined above. The concentration of the luminescent species in the UV-curable fluoropolymer was varied between 0 wt% and 10 wt%. Each sealed DSSC was fixed onto a SPIN150 spin processor (SPS-Europe), and a few drops of the UV-curable reactive mixture were placed on the external side of the photoanode. Samples were spin-coated at 1000 rpm for 40 s with an acceleration equal to 25 rpm s^{-1}, and subsequently UV-cured with the above described procedure. The final thickness of the coating was 30 μm, which preliminary tests proved to be the best value for these purposes (see Table S1 in the Supporting Information).

Characterization Techniques: UV–vis and fluorescence spectroscopy were performed on photocrosslinked LDS films deposited onto glass/quartz substrates by spin-coating (WS-400B-NPP Spin-Processor, Laurell Technologies Corp.) at 1000 rpm for 40 s in air. UV–vis absorption spectra were recorded in air at room temperature in transmission mode by means of an Evolution 600 UV–vis Spectrophotometer (Thermo Scientific). Fluorescence emission spectra were recorded in air at room temperature on a Jasco FP-6600 spectrofluorometer. The excitation wavelength was λ_{exc} = 340 nm. FTIR spectroscopy was used to monitor the reaction for the synthesis of the photocrosslinkable precursor. FTIR spectra were recorded in air at room temperature with a Nicolet 670-FTIR spectrophotometer. DSC was performed on solid state samples using a Mettler-Toledo DSC/823^e instrument at a scan rate of 20 °C min^{-1} in nitrogen environment. TGA was performed on solid state samples using a Q500 TGA system (TA Instruments) from ambient temperature to 600 °C at a scan rate of 10 °C min^{-1} in air. Static optical contact angle measurements on the LDS coating were performed with an OCA 20 (DataPhysics) equipped with a CCD photo-camera and with a 500-µL Hamilton syringe to dispense liquid droplets. Measurements were taken at room temperature *via* the sessile drop technique. At least 20 measurements were performed in different regions on the surface of each coating and results were averaged. Water and diiodomethane were used as probe liquids. PV measurements were performed on DSSC devices having active area of 0.78 cm^2 using a 0.16 cm^2 rigid black mask. *I–V* electrical characterizations under AM1.5G illumination (100 mW cm^{-2}, or 1 sun) were carried out using a class A solar simulator (91195A, Newport) and a Keithley 2440 source measure unit. All the measurements were carried out on at least three different fresh cells in order to verify the reproducibility of the obtained results, and the experimental results shown in the manuscript are the average of the three replicates. IPCE measurements were performed in DC mode using a 100-W QTH lamp (Newport) as light source and a 150-mm Czerny Turner monochromator (Omni-λ 150, Lot-Oriel, Darmstadt, Germany).

Supporting Information

Supporting Information is available from the Wiley Online Library or from the author.

Acknowledgements

G.G. gratefully acknowledges Gigliola Clerici for support with thermal analysis measurements.

[1] a) B. O'Regan, M. Grätzel, *Nature* **1991**, *353*, 737; b) M. Grätzel, *J. Photochem. Photobiol., C* **2003**, *4*, 145.
[2] a) P. Docampo, S. Guldin, T. Leijtens, N. K. Noel, U. Steiner, H. J. Snaith, *Adv. Mater.* **2014**, *26*, 4013; b) A. Hagfeldt, G. Boschloo, L. C. Sun, L. Kloo, H. Pettersson, *Chem. Rev.* **2010**, *110*, 6595.
[3] H. F. Sun, T. T. Pan, G. Q. Hu, Y. W. Sun, D. T. Wang, X. X. Zhang, *Prog. Chem.* **2014**, *26*, 609.
[4] D. Kuang, S. Uchida, R. Humphry-Baker, S. M. Zakeeruddin, M. Grätzel, *Angew. Chem. Int. Ed.* **2008**, *47*, 1923.
[5] a) S. Mathew, A. Yella, P. Gao, R. Humphry-Baker, B. F. E. Curchod, N. Ashari-Astani, I. Tavernelli, U. Rothlisberger, M. K. Nazeeruddin, M. Grätzel, *Nat. Chem.* **2014**, *6*, 242; b) S. Ahmad, E. Guillen, L. Kavan, M. Grätzel, M. K. Nazeeruddin, *Energy Environ. Sci.* **2013**, *6*, 3439; c) P. Gao, H. N. Tsao, C. Yi, M. Grätzel, M. K. Nazeeruddin, *Adv. Energy Mater.* **2014**, *4*, 1301485.
[6] a) K. J. Jiang, K. Manseki, Y. H. Yu, N. Masaki, J. B. Xia, L. M. Yang, Y. L. Song, S. Yanagida, *New J. Chem.* **2009**, *33*, 1973; b) C. J. Jiao, N. N. Zu, K. W. Huang, P. Wang, J. S. Wu, *Org. Lett.* **2011**, *13*, 3652; c) A. Mishra, M. K. R. Fischer, P. Bauerle, *Angew. Chem. Int. Ed.* **2009**, *48*, 2474; d) K. Kakiage, Y. Aoyama, T. Yano, T. Otsuka, T. Kyomen, M. Unno, M. Hanaya, *Chem. Commun.* **2014**, *50*, 6379.
[7] a) J. M. Ball, N. K. S. Davis, J. D. Wilkinson, J. Kirkpatrick, J. Teuscher, R. Gunning, H. L. Anderson, H. J. Snaith, *RSC Adv.* **2012**, *2*, 6846; b) A. Abate, M. Planells, D. J. Hollman, S. D. Stranks, A. Petrozza, A. R. S. Kandada, Y. Vaynzof, S. K. Pathak, N. Robertson, H. J. Snaith, *Adv. Energy Mater.* **2014**, *4*, 1400116.
[8] a) T. Horiuchi, H. Miura, K. Sumioka, S. Uchida, *J. Am. Chem. Soc.* **2004**, *126*, 12218; b) S. Ito, H. Miura, S. Uchida, M. Takata, K. Sumioka, P. Liska, P. Comte, P. Pechy, M. Grätzel, *Chem. Commun.* **2008**, 5194.
[9] B. E. Hardin, E. T. Hoke, P. B. Armstrong, J. H. Yum, P. Comte, T. Torres, J. M. J. Fréchet, M. K. Nazeeruddin, M. Grätzel, M. D. McGehee, *Nat. Photonics* **2009**, *3*, 406.
[10] a) C. M. Lan, H. P. Wu, T. Y. Pan, C. W. Chang, W. S. Chao, C. T. Chen, C. L. Wang, C. Y. Lin, E. W. G. Diau, *Energy Environ. Sci.* **2012**, *5*, 6460; b) A. Yella, H. W. Lee, H. N. Tsao, C. Y. Yi, A. K. Chandiran, M. K. Nazeeruddin, E. W. G. Diau, C. Y. Yeh, S. M. Zakeeruddin, M. Grätzel, *Science* **2011**, *334*, 629; c) H. P. Wu, Z. W. Ou, T. Y. Pan, C. M. Lan, W. K. Huang, H. W. Lee, N. M. Reddy, C. T. Chen, W. S. Chao, C. Y. Yeh, E. W. G. Diau, *Energy Environ. Sci.* **2012**, *5*, 9843; d) L. L. Li, E. W. G. Diau, *Chem. Soc. Rev.* **2013**, *42*, 291.
[11] R. Y. Ogura, S. Nakane, M. Morooka, M. Orihashi, Y. Suzuki, K. Noda, *Appl. Phys. Lett.* **2009**, *94*, 073308.
[12] A. Ehret, L. Stuhl, M. T. Spitler, *J. Phys. Chem. B* **2001**, *105*, 9960.
[13] a) Y. Li, K. Pan, G. F. Wang, B. J. Jiang, C. G. Tian, W. Zhou, Y. Qu, S. Liu, L. Feng, H. G. Fu, *Dalton Trans.* **2013**, *42*, 7971; b) J. L. Wang, J. H. Wu, J. M. Lin, M. L. Huang, Y. F. Huang, Z. Lan, Y. M. Xiao, G. T. Yue, S. Yin, T. Sato, *ChemSusChem* **2012**, *5*, 1307; c) D. K. Yim, I. S. Cho, S. Lee, C. H. Kwak, D. H. Kim, J. K. Lee, K. S. Hong, *J. Nanosci. Nanotechnol.* **2011**, *11*, 8748; d) Q. B. Li, J. M. Lin, J. H. Wu, Z. Lan, J. L. Wang, Y. Wang, F. G. Peng, M. L. Huang, Y. M. Xiao, *Chin. Sci. Bull.* **2011**, *56*, 3114; e) C. K. Hong, H. S. Ko, E. M. Han, J. J. Yun, K. H. Park, *Nanoscale Res. Lett.* **2013**, *8*.
[14] D. Xiong, W. Chen, *Front. Optoelectron.* **2012**, *5*, 371.
[15] M. Durr, A. Bamedi, A. Yasuda, G. Nelles, *Appl. Phys. Lett.* **2004**, *84*, 3397.
[16] a) J. Usagawa, S. S. Pandey, S. Hayase, M. Kono, Y. Yamaguchi, *Appl. Phys. Express* **2009**, *2*; b) S. Q. Fan, B. Fang, H. Choi, S. Paik, C. Kim, B. S. Jeong, J. J. Kim, J. Ko, *Electrochim. Acta* **2010**, *55*, 4642; c) M. Yanagida, N. Onozawa-Komatsuzaki, M. Kurashige, K. Sayama, H. Sugihara, *Sol. Energy Mater. Sol. Cells* **2010**, *94*, 297.
[17] Z. Hosseini, W. K. Huang, C. M. Tsai, T. M. Chen, N. Taghavinia, E. W. G. Diau, *ACS Appl. Mater. Interfaces* **2013**, *5*, 5397.
[18] G. Mincuzzi, L. Vesce, M. Schulz-Ruthenberg, E. Gehlen, A. Reale, A. Di Carlo, T. M. Brown, *Adv. Energy Mater.* DOI: 10.1002/aenm.201400421.
[19] E. Klampaftis, D. Ross, K. R. McIntosh, B. S. Richards, *Sol. Energy Mater. Sol. Cells* **2009**, *93*, 1182.
[20] a) E. Klampaftis, B. S. Richards, *Prog. Photovoltaics* **2011**, *19*, 345; b) D. Ross, E. Klampaftis, J. Fritsche, M. Bauer, B. S. Richards, *Sol. Energy Mater. Sol. Cells* **2012**, *103*, 11.
[21] a) B. S. Richards, *Sol. Energy Mater. Sol. Cells* **2006**, *90*, 1189; b) B. S. Richards, K. R. McIntosh, *Prog. Photovoltaics* **2007**, *15*, 27; c) D. Alonso-Álvarez, D. Ross, E. Klampaftis, K. R. McIntosh, S. Jia, P. Storiz, T. Stolz, B. S. Richards, *Prog. Photovoltaics* DOI: 10.1002/pip.2462; d) E. Klampaftis, D. Ross, S. Seyrling, A. N. Tiwari, B. S. Richards, *Sol. Energy Mater. Sol. Cells* **2012**, *101*, 62.

[22] X. Sheng, C. J. Corcoran, J. W. He, L. Shen, S. Kim, J. Park, R. G. Nuzzo, J. A. Rogers, *Phys. Chem. Chem. Phys.* **2013**, *15*, 20434.

[23] a) K. R. McIntosh, G. Lau, J. N. Cotsell, K. Hanton, D. L. Batzner, F. Bettiol, B. S. Richards, *Prog. Photovoltaics* **2009**, *17*, 191; b) T. Maruyama, Y. Shinyashiki, S. Osako, *Sol. Energy Mater. Sol. Cells* **1998**, *56*, 1; c) C. K. Huang, Y. C. Chen, W. B. Hung, T. M. Chen, K. W. Sun, W. L. Chang, *Prog. Photovoltaics* **2013**, *21*, 1507.

[24] a) M. N. Huang, Y. Y. Ma, F. Xiao, Q. Y. Zhang, *Spectrochim. Acta, Part A* **2014**, *120*, 55; b) M. N. Huang, Y. Y. Ma, X. Y. Huang, S. Ye, Q. Y. Zhang, *Spectrochim. Acta, Part A* **2013**, *115*, 767.

[25] a) M. Zahedifar, Z. Chamanzadeh, S. M. H. Mashkani, *J. Lumin.* **2013**, *135*, 66; b) D. D. Wu, Y. Q. Ma, X. Zhang, S. B. Qian, G. H. Zheng, M. Z. Wu, G. Li, Z. Q. Sun, *J. Rare Earths* **2012**, *30*, 325; c) X. Y. Huang, J. X. Wang, D. C. Yu, S. Ye, Q. Y. Zhang, X. W. Sun, *J. Appl. Phys.* **2011**, *109*, 113526.

[26] J. F. Liu, Q. H. Yao, Y. D. Li, *Appl. Phys. Lett.* **2006**, *88*, 173119.

[27] a) F. Bella, R. Bongiovanni, R. S. Kumar, M. A. Kulandainathan, A. M. Stephan, *J. Mater. Chem. A* **2013**, *1*, 9033; b) A. Chiappone, F. Bella, J. R. Nair, G. Meligrana, R. Bongiovanni, C. Gerbaldi, *ChemElectroChem* **2014**, *1*, 1350. c) G. Griffini, S. Turri, M. Levi, *Polym. Bull.* **2011**, *66*, 211.

[28] a) S. K. Pathak, A. Abate, T. Leijtens, D. J. Hollman, J. l. Teuscher, L. Pazos, P. Docampo, U. Steiner, H. J. Snaith, *Adv. Energy Mater.* **2014**, *4*, 1301667; b) S. B. Hong, S. H. Park, J. H. Kim, S. Y. Lee, Y. S. Kwon, T. Park, P. H. Kang, S. C. Hong, *Adv. Energy Mater.* **2014**, *4*, 1400477.

[29] a) L. Yao, J. H. He, *Prog. Mater. Sci.* **2014**, *61*, 94; b) R. M. Fillion, A. R. Riahi, A. Edrisy, *Renewable Sustainable Energy Rev.* **2014**, *32*, 797; c) W. L. Min, B. Jiang, P. Jiang, *Adv. Mater.* **2008**, *20*, 3914; d) S. F. Pellicori, C. L. Martinez, P. Hausgen, D. Wilt, *Appl. Opt.* **2014**, *53*, A339; e) S. H. Lee, K. S. Han, J. H. Shin, S. Y. Hwang, H. Lee, *Prog. Photovoltaics* **2013**, *21*, 1056; f) P. Siffalovic, M. Jergel, M. Benkovicova, A. Vojtko, V. Nadazdy, J. Ivanco, M. Bodik, M. Demydenko, E. Majkova, *Sol. Energy Mater. Sol. Cells* **2014**, *125*, 127.

[30] a) G. Griffini, M. Levi, S. Turri, *Prog. Org. Coat.* **2014**, *77*, 528; b) G. Griffini, M. Levi, S. Turri, *Sol. Energy Mater. Sol. Cells* **2013**, *118*, 36.

[31] a) S. Y. Heo, J. K. Koh, G. Kang, S. H. Ahn, W. S. Chi, K. Kim, J. H. Kim, *Adv. Energy Mater.* **2014**, *4*, 1300632; b) J. T. Park, J. H. Kim, D. Lee, *Nanoscale* **2014**, *6*, 7362.

[32] F. Bella, A. Sacco, G. P. Salvador, S. Bianco, E. Tresso, C. F. Pirri, R. Bongiovanni, *J. Phys. Chem. C* **2013**, *117*, 20421.

[33] ASTM D5402–93, *Standard practice for assessing the solvent resistance of organic coatings using solvent rubs*, **1999**.

[34] a) R. S. Fontenot, W. A. Hollerman, K. N. Bhat, M. D. Aggarwal, *J. Lumin.* **2012**, *132*, 1812; b) R. S. Fontenot, K. N. Bhat, W. A. Hollerman, M. D. Aggarwal, K. M. Nguyen, *CrystEngComm* **2012**, *14*, 1382.

[35] a) S. Morita, M. Ikegami, T. C. Wei, T. Miyasaka, *ChemPhysChem* **2014**, *15*, 1190; b) X. J. Chen, D. Xu, L. H. Qiu, S. C. Li, W. Zhang, F. Yan, *J. Mater. Chem. A* **2013**, *1*, 8759.

[36] a) A. Hilmi, T. A. Shoker, T. H. Ghaddar, *ACS Appl. Mater. Interfaces* **2014**, *6*, 8744; b) M. Afrooz, H. Dehghani, *J. Power Sources* **2014**, *262*, 140.

[37] S. R. Raga, F. Fabregat-Santiago, *Phys. Chem. Chem. Phys.* **2013**, *15*, 2328.

[38] a) J. Scheirs, *Modern Fluoropolymers: High Performance Polymers for Diverse Applications* John Wiley & Sons Ltd, Chichester, UK **1997**; b) G. Hougham, P. E. Cassidy, K. Johns, T. Davidson, *Fluoropolymers 2. Properties* Kluwer Academic/Plenum Publishers, New York **1999**.

[39] M. Giannouli, G. Syrrokostas, P. Yianoulis, *Prog. Photovoltaics* **2010**, *18*, 128.

[40] ARPA Piemonte (Regional agency for environmental protection) website, http://www.arpa.piemonte.it/rischinaturali/tematismi/clima/rapporti-di-analisi/Eventi.html, (accessed June 2014).

[41] N. Kayaman-Apohan, R. Demirci, M. Cakir, A. Gungor, *Radiat. Phys. Chem.* **2005**, *73*, 254.

[42] a) W. C. Lin, C. H. Yang, T. L. Wang, Y. T. Shieh, W. J. Chen, *eXPRESS Polym. Lett.* **2012**, *6*, 2; b) L. J. Chen, Q. L. Tai, L. Song, W. Y. Xing, G. X. Jie, Y. Hu, *eXPRESS Polym. Lett.* **2010**, *4*, 539.

[43] a) Y. T. Shieh, H. T. Chen, K. H. Liu, Y. K. Twu, *J. Polym. Sci., Part A: Polym. Chem.* **1999**, *37*, 4126; b) I. Mita, in *Aspects of Degradation and Stabilization of Polymers* (Ed: H. H. G. Jellinek), Elsevier Scientific Publishing Company, Amsterdam, The Netherlands **1978**, Ch. 6.

[44] a) A. Alaaeddine, F. Boschet, B. Ameduri, B. Boutevin, *J. Polym. Sci., Part A: Polym. Chem.* **2012**, *50*, 3303; b) G. Couture, B. Campagne, A. Alaaeddine, B. Ameduri, *Polym. Chem.* **2013**, *4*, 1960; c) G. Tillet, P. De Leonardis, A. Alaaeddine, M. Umeda, S. Mori, N. Shibata, S. M. Aly, D. Fortin, P. D. Harvey, B. Ameduri, *Macromol. Chem. Phys.* **2012**, *213*, 1559.

[45] S. Wu, *J. Colloid Interface Sci.* **1979**, *71*, 605.

[46] J. H. Yum, P. Walter, S. Huber, D. Rentsch, T. Geiger, F. Nuesch, F. De Angelis, M. Grätzel, M. K. Nazeeruddin, *J. Am. Chem. Soc.* **2007**, *129*, 10320.

[47] T. Kitamura, K. Okada, H. Matsui, N. Tanabe, *J. Sol. Energy Eng.* **2010**, *132*.

[48] B. Macht, M. Turrion, A. Barkschat, P. Salvador, K. Ellmer, H. Tributsch, *Sol. Energy Mater. Sol. Cells* **2002**, *73*, 163.

[49] C. Chen, X. C. Yang, M. Cheng, F. G. Zhang, L. C. Sun, *ChemSusChem* **2013**, *6*, 1270.

[50] G. Griffini, J. D. Douglas, C. Piliego, T. W. Holcombe, S. Turri, J. M. J. Fréchet, J. L. Mynar, *Adv. Mater.* **2011**, *23*, 1660.